Examples of Quantum Dynamics in Optomechanical Systems

Max Ludwig, Georg Heinrich, and Florian Marquardt

Arnold-Sommerfeld Center for Theoretical Physics, Center for NanoScience and Department of Physics, Ludwig-Maximilians Universität München, Munich, Germany

Abstract. Optomechanical systems exploit the interaction between the optical radiation field and mechanical resonators in a laser-driven cavity. In the past few years, these systems have been the focus of considerable experimental and theoretical attention, yielding promising successes, particularly in using optomechanical cooling to reduce the thermal occupation of the resonators. This offers the prospect of observing quantum dynamics involving the motion of macroscopic mechanical objects. We review two features: First, the nonlinear self-induced mechanical oscillations induced by a strong laser drive can exhibit interesting quantum behaviour at low temperatures. Second, a mechanically driven membrane inside an optical cavity can 'shuttle photons' around, and this system exhibits intricate dynamical interference effects (Landau-Zener-Stueckelberg oscillations).

Keywords: Optomechanics, quantum electrodynamics, quantum physics, photons, nanomechanics, optical cavity.

1 Introduction

The interaction of light with matter is one of the fundamental topics in physics. A new chapter has been opened by the recent combination of nano- and micromechanical systems with optical cavities. The light circulating inside the cavity exerts a radiation pressure force on a moveable mirror (attached to the mechanical resonator), thus inducing mechanical motion. Conversely, any motion results in a change of the cavity length, displacing the optical resonance frequency, and thus influencing the circulating intensity, i.e. the force. In this way, an interesting coupled dynamics of the light field and the mechanical vibration is produced. Among other effects, the light can be used to cool the mechanical motion (in analogy to laser cooling of atoms). This has been exploited to cool mechanical resonators to near the ground state of the mechanical motion of one of their vibrational eigenmodes (for recent experimental examples see [1,2]). Once ground state cooling is achieved, a wealth of quantum effects may be observed, creating nonclassical states in optomechanical systems. We refer the reader to our recent review [3] for a non-technical introduction and comprehensive references to the literature.

A. Sergienko, S. Pascazio, and P. Villoresi (Eds.): QuantumCom 2009, LNICST 36, pp. 167–179, 2010.

In the present contribution, we discuss and review our results concerning two topics connected to the dynamics of optomechanical systems.

First, we discuss the nonlinear self-induced mechanical oscillations induced by a strong laser drive that can exhibit interesting quantum behaviour at low temperatures. When the laser beam is blue detuned with respect to the cavity, the back-action of the light onto the mechanical motion tends to diminish the mechanical damping rate. This can lead to an instability which makes the system settle into a pattern of periodic oscillations. The power dissipated by intrinsic mechanical friction is then offset by the power fed into the system via the radiation. We have analyzed theoretically the behaviour in this regime for a system cooled down to low temperatures, into the quantum regime of mechanical motion. Using a master equation description, we have found the quantum state of the oscillator, taking full account of the effects of quantum fluctuations.

Second, a mechanically driven membrane inside an optical cavity can 'shuttle photons' around, and this system exhibits intricate dynamical interference effects. When a partially transparent membrane is placed between two fixed end-mirrors, it essentially divides the cavity in two halves. Photons then can tunnel through the membrane from one side to the other. A photon being in the left or the right side of the cavity realizes a simple two-state system. When applying a mechanical drive to the membrane, one can shuttle photons from the left half to the right half, which shows up in the amount of light transmitted through the whole setup. When the drive is too fast for this regular shuttle process, one can see interesting interference phenomena. Essentially, this setup thus allows to observe the physics of driven two-level systems in an optomechanical setting. This includes, in particular, interference effects at stronger drive, known as Landau-Zener-Stueckelberg oscillations.

2 Quantum Nonlinear Dynamics in Optomechanical Systems

The delayed light force in an optomechanical system changes the mechanical damping rate. The additional contribution Γ_{opt} can become negative, decreasing the total damping rate Γ_{full}. When Γ_{full} becomes negative as well, the system settles into a nonlinear dynamical regime of self-sustained oscillations [4,5]. In this section, we will describe the quantum behaviour in this regime. An extensive previous analysis has been published in [5]. We will illustrate the main features by some additional numerical examples not to be found in [5].

2.1 The Model

In the following we will focus on comparing the quantum dynamics of the coupled cavity-oscillator system to the results of the analytic solution of the classical equations of motion. In doing so we will discuss the effect of quantum fluctuations and identify a quantum parameter that allows to keep track of the quantum-to-classical transition. In particular we will present results of a fully quantum

mechanical approach based on a master equation in Lindblad form, and results of a semi-classical approach based on Langevin equations where quantum effects are mimicked by fluctuating noise terms.

We consider the following Hamiltonian to describe a generic optomechanical system consisting of a driven optical cavity whose resonance frequency depends on the position of a mechanical element:

$$\begin{aligned}\hat{H} = \hbar\left(-\Delta + g_M\left(\hat{b}+\hat{b}^\dagger\right)\right)\hat{a}^\dagger\hat{a} \;+\; \hbar\omega_M\hat{b}^\dagger\hat{b} \;+ \\ \hbar\alpha_L(\,\hat{a}+\hat{a}^\dagger\,) \;+\; \hat{H}_\kappa \;+\; \hat{H}_{\Gamma_M} \;=\; \hat{H}_0 \;+\; \hat{H}_\kappa \;+\; \hat{H}_{\Gamma_M}\,,\end{aligned} \tag{1}$$

which is written in the rotating frame of the driving laser field whose frequency is denoted by ω_L and whose amplitude is set by α_L. The laser is detuned by $\Delta = \omega_L - \omega_{\rm cav}$ with respect to the optical cavity mode which is described by photon annihilation and creation operators $\hat{a}$ and $\hat{a}^\dagger$. The mechanical oscillator is characterized by its frequency ω_M and mass m_M, and its displacement is given by $\hat{x}_M = x_{\rm ZPF}(\hat{b}+\hat{b}^\dagger)$, with a mechanical zero-point amplitude of $x_{\rm ZPF} = \sqrt{\hbar/(2m_M\omega_M)}$. The optomechanical coupling, i.e. the coupling between the optical field and the mechanical displacement, is given by the parameter g_M. In the simplest case, with a movable, fully reflecting mirror at one end of an optical cavity of length L, we have $g_M = -\omega_{\rm cav}x_{\rm ZPF}/L$, and thus $g_M(\hat{b}+\hat{b}^\dagger) = -\omega_{\rm cav}\hat{x}_M/L$. The radiation pressure force corresponding to this coupling term is given by $\hat{F}_{\rm rad} = -\hbar g_M\hat{a}^\dagger\hat{a}/x_{\rm ZPF} = \hbar\omega_{\rm cav}\hat{a}^\dagger\hat{a}/L$. The decay of the cavity photons and the mechanical damping of the cantilever are captured by $\hat{H}_\kappa$ with a cavity ring down rate κ, and by $\hat{H}_{\Gamma_M}$ with a damping rate Γ_M, respectively.

2.2 Classical Dynamics

The classical equations of motion following from the Hamiltonian (1) can be rescaled (see ref. [5]) to

$$\begin{aligned}\frac{d\tilde{\alpha}}{d\tilde{t}} &= [i(\frac{\Delta}{\omega_M}+\tilde{x}) - \frac{1}{2}\frac{\kappa}{\omega_M}]\tilde{\alpha} + \frac{1}{2} \\ \frac{d^2\tilde{x}}{d\tilde{t}^2} &= -\tilde{x} + \mathcal{P}\,|\tilde{\alpha}|^2 - \frac{\Gamma_M}{\omega_M}\frac{d\tilde{x}}{d\tilde{t}}\,,\end{aligned} \tag{2}$$

where $\tilde{t} = \omega_M t$, $\tilde{\alpha} = i\alpha\omega_M/(2\alpha_L)$, $\tilde{x} = gx/(\omega_M x_{\rm ZPF})$ and the field operator $\hat{a}$ is replaced by the classical amplitude α and the position operator $\hat{x}$ by the classical quantity x. Note that the system's dynamics is governed by four dimensionless parameters only, the driving strength $\mathcal{P} = 8|\alpha_L|^2 g_M^2/\omega_M^4$, the detuning Δ/ω_M, the cavity decay κ/ω_M and the mechanical dissipation Γ_M/ω_M, and that it is purely deterministic as both photon shot noise and mechanical fluctuations are ignored.

Above a certain threshold of driving power the mechanical resonator will perform self-sustained oscillations of the form $x(t) \approx \bar{x} + A\cos(\omega_M t)$ in steady state, as has been seen experimentally [6,7,8]. Hence the oscillator's dynamics is fully determined once the parameters $\{\bar{x}, A\}$ are found as a function of

$\{\mathcal{P}, \Delta/\omega_M, \kappa/\omega_M, \Gamma_M/\omega_M\}$. This task, as presented in detail in [4,5], is accomplished by demanding that, firstly, the total force on the mechanical resonator has to vanish on average, and, secondly, the power transferred to the mechanical resonator from the light field has to balance the friction loss, i.e. $P_{\mathrm{rad}}/P_{\mathrm{fric}} \equiv 1$.

Hence after eliminating $\bar{x}$ from the force balance condition, the attractors for the oscillation amplitude A or equivalently for the oscillation energy $E_{M,\mathrm{cl}} = \frac{1}{2}m\omega_M^2 A^2$, can be determined implicitly from the power balance condition as demonstrated in Figure 1(a): The plot shows the ratio $P_{\mathrm{rad}}/P_{\mathrm{fric}}$ as a function of detuning Δ/ω_M and oscillation energy $E_{\mathrm{M,cl}}$. The contour lines correspond to $P_{\mathrm{rad}}/P_{\mathrm{fric}} \equiv 1$ for different values of the mechanical damping rate and represent solutions of the oscillation energy (and thus A) as a function of Δ/ω_M for given values of $\mathcal{P} = 0.12$, $\kappa/\omega_M = 0.3$ and $\Gamma_M/\omega_M = 0.074$ (black), 0.071 (blue), 0.019 (white). Note that the oscillation energy E_M is scaled by a characteristic energy scale of the system, $E_0 = \frac{1}{2}m\omega_M^2 x_{\mathrm{FWHM}}^2$, where x_{FWHM}denotes the full width at half maximum (FWHM) of the cavity translated into a length scale ($x_{FWHM} = \kappa L/\omega_{\mathrm{cav}}$, where L is the cavity's length).

For $\kappa < \omega_M$ the attractor diagram shows pronounced features at the sidebands, where the detuning Δ equals an integer multiple of the mechanical frequency ω_M. However, due to the large driving power $\mathcal{P}$, the resonance peaks are strongly tilted, shifted towards lower detunings and show discontinuities. At the second sideband the strongly damped solution (black contour) does not feature self-oscillations. After a small reduction of the damping rate, however, the attractor at the second sideband appears, i.e. oscillations at finite amplitude (blue line) are possible solutions of the system. Because $A = 0$ remains to be a stable solution at the second sideband, the system already shows bistable behaviour (and, more generally, multistable behaviour for other parameter sets).

2.3 The Quantum Parameter

In contrast to the classical equations of motion, the set of parameters, $\mathcal{P}, \Delta/\omega_M$, κ/ω_M, Γ_M/ω_M does not suffice for a quantum mechanical treatment, where $\hbar$ enters as well. The quantum mechanical nature of the system can be described by a "quantum parameter" ζ, which compares the magnitude of the cantilever's zero-point fluctuations, x_{ZPF}, with the cavity linewidth x_{FWHM}:

$$\text{quantum parameter} : \zeta = \frac{x_{\mathrm{ZPF}}}{x_{\mathrm{FWHM}}} = \frac{g_M}{\kappa}. \tag{3}$$

Obviously, this turns out to be equal to the ratio of the optomechanical coupling frequency g_M and the cavity decay rate κ, such that values larger than one indicate a strong-coupling regime. The quantum parameter ζ vanishes in the classical limit $\hbar \to 0$, as the zero-point fluctuations x_{ZPF} of the cantilever go to zero. The magnitude of ζ determines the effect of quantum fluctuations, i.e. the shot noise of the cavity and the mechanical zero-point fluctuations on the dynamics of the coupled cavity-cantilever system.

We note that there is an alternative way to introduce the quantum parameter (3) by comparing the mechanical zero-point momentum fluctuations to the momentum a single intracavity photon transfers to the cantilever. This approach

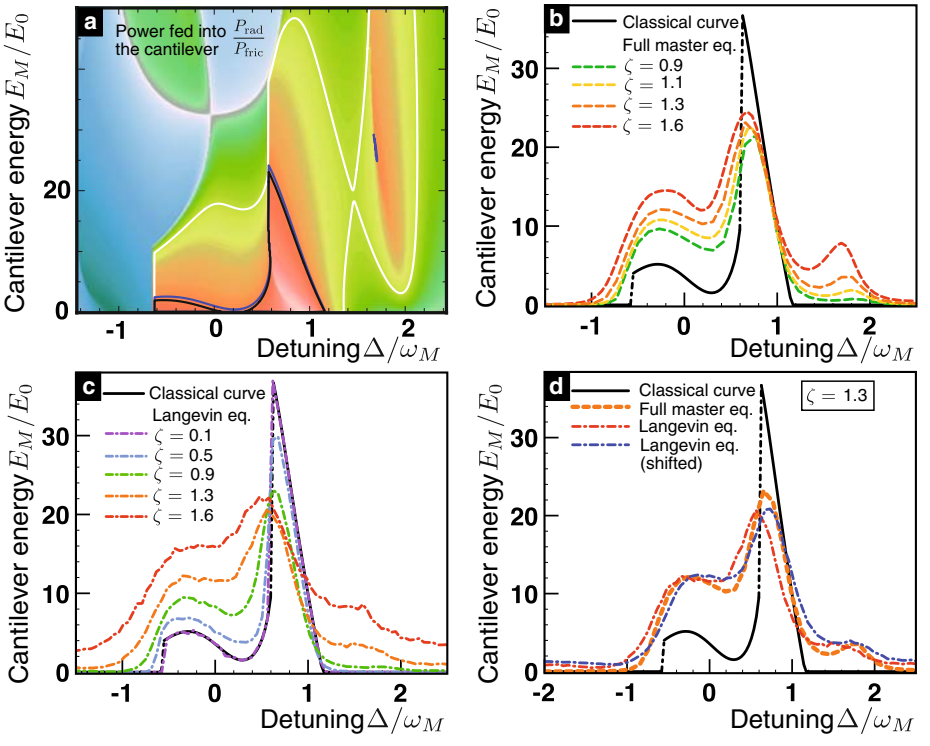

Fig. 1. Self-induced optomechanical oscillations in the quantum regime. Plots of cantilever oscillation energy vs. detuning for various parameters. Results from the Langevin equation (which mimicks quantum noise) are compared to the purely deterministic classical solution and to the results from the full quantum master equation. The parameters are $\kappa/\omega_M = 0.3$, $\Gamma_M = 0.074$, $\mathcal{P} = 0.12$. (a) The classical solution for the oscillation energy is given by the black contour line in the attractor diagram, while the blue (gray) and white contours depict the solutions for lower damping rates, $\Gamma_M = 0.071$ and $\Gamma_M = 0.019$ respectively. Self-oscillations at the second sideband occur already for slightly modified parameters (see the blue contour line). (b) In the solutions of the full quantum master equation (dashed curves), we observe a shift of the resonances towards lower detunings and a smooth behaviour, in contrast to the sharp structures and discontinuities of the classical result (black curve). For high values of the quantum parameter ζ [see main text], the quantum curves show features that occur in the classical solution for lower damping rates only: The peak at the second sideband appears and the peaks of the first and second sideband merge. (c) The results of the Langevin equation recover the classical curves for the case of very weak quantum fluctuations, i.e. for $\zeta = 0.1$. They also reproduce the main features of the curves that come from the master equation. However, this approach fails to match the results of the master equation for large values of ζ and outside the region of instability. (d) Replacing the radiation pressure term of equation (7) by $\frac{\hbar g}{m x_{\rm ZPF}}(|\alpha|^2 - \frac{1}{2})$ shifts the semi-classical curve towards lower detunings, but does not lead to a better agreement with the curve from the quantum master equation.

has been presented in [9] where the mechanical element was composed of an ensemble of ultracold atoms. When the photon is reflected at the mechanical oscillator, it transfers a momentum of $2\hbar k$. This process is repeated after one cavity round-trip time $\frac{2L}{c}$ for as long as the photon stays inside the cavity, i.e. for a span of time given by κ^{-1}. The total transfer of momentum is therefore given by $p_{\mathrm{phot}} = \hbar k \frac{c}{L}\kappa^{-1} = \hbar\omega_{\mathrm{cav}}/\kappa L$. The strength of the zero-point momentum fluctuations is given by $p_{\mathrm{ZPF}} = \sqrt{\frac{\hbar m_M \omega_M}{2}} = \frac{\hbar}{2x_{\mathrm{ZPF}}}$. Taking the ratio of these two quantities leads directly to the quantum parameter:

$$\frac{p_{\mathrm{phot}}}{p_{\mathrm{ZPF}}} = \frac{2x_{\mathrm{ZPF}}}{\kappa L/\omega_{\mathrm{cav}}} = 2\zeta. \tag{4}$$

We see that for a large quantum parameter a single phonon of the cantilever causes a detectable shift of the cavity resonance. In turn, a single photon causes the cantilever to change its momentum noticeably.

2.4 Quantum Dynamics: Master Equation

We will now investigate the quantum dynamics in the regime of self-induced oscillations. We choose to focus on the extreme quantum regime, where the bath temperature is set to zero and the quantum parameter is made to achieve values around one. This demonstrates the effects of quantum fluctuations most clearly. Although this limit cannot be reached (at present) using micro- or nanomechanical resonators (where bulk temperatures are high and the quantum parameter is less than 10^{-3}), it might be achievable in cold atom systems or other variants.

For a fully quantum mechanical treatment we aim at finding the steady state solution of the reduced density matrix $\hat{\rho}$ for the mechanical oscillator and the optical mode of the cavity. The time evolution of $\hat{\rho}$ is given by

$$\frac{d}{dt}\hat{\rho} = \frac{[\hat{H}_0, \hat{\rho}]}{i\hbar} + \Gamma_M \mathcal{D}[\hat{b}] + \kappa \mathcal{D}[\hat{a}], \tag{5}$$

where $\mathcal{D}[\hat{A}] = \hat{A}\hat{\rho}\hat{A}^\dagger - \frac{1}{2}\hat{A}^\dagger\hat{A}\hat{\rho} - \frac{1}{2}\hat{\rho}\hat{A}^\dagger\hat{A}$ denotes the standard Lindblad operator and we assumed the mechanical bath to be at zero temperature.

For the numerical evaluation, we rewrite equation 5 as $d\hat{\rho}/dt = \mathcal{L}\hat{\rho}$, with a Liouvillian super-operator $\mathcal{L}$. We then interpret the density matrix as a vector with a finite length in a truncated Fock-state basis of the coupled system. The time evolution of $\hat{\rho}$ is then governed by the matrix $\mathcal{L}$ and the density matrix at long times (in steady state) is given by the eigenvector of $\mathcal{L}$ with eigenvalue 0. The numerical calculation of this eigenvector is much more efficient than a simulation of the full time evolution. Since we are dealing with large sparse matrices, it is convenient to employ an Arnoldi method that finds a few eigenvalues and eigenvectors of $\mathcal{L}$ by iterative projection. For Hermitean matrices, the Arnoldi method is also known as the Lanczos algorithm.

For a comparison with the classical solution, the mechanical energy is evaluated from the system's steady state density matrix as $E_{M,\mathrm{qm}} = \hbar\omega_M \langle \hat{n}_M \rangle =$

$\hbar\omega_M \mathrm{Tr}(\hat{n}_M\hat{\rho})$. Note that we exclude the zero-point energy and define the occupation number operator as $\hat{n}_M = \hat{b}^\dagger\hat{b} + \frac{1}{4x_{\mathrm{ZPF}}^2}\big(\langle\hat{x}_M\rangle^2 - 2\hat{x}_M\langle\hat{x}_M\rangle\big)$ in order to exclude the effects of a static displacement of the mechanical resonator, i.e. $\langle\hat{x}_M\rangle \neq 0$. Only in this case the expectation value of $\hat{n}_M$ corresponds to the oscillation energy. The scale of the mechanical energy is again set by the classical quantity $E_0 = \frac{1}{2}m\omega_M^2 x_{\mathrm{FWHM}}^2$ such that $E_M/E_0 = 4\zeta^2\langle\hat{n}_M\rangle$.

In figure 1(b) we demonstrate the influence of the quantum parameter $\zeta = x_{\mathrm{ZPF}}/x_{\mathrm{FWHM}}$ determining the crossover from the quantum regime towards classical behaviour. In particular we compare the oscillation energy obtained from the classical solution to the results coming from the master equation approach. The classical (black) curve depicts the oscillation energy as a function of the detuning parameter and corresponds to the black contour in the attractor diagram. It features self-oscillations around the resonance ($\Delta = 0$) and the first sideband ($\Delta/\omega_M = 1$) and discontinuities at the left slopes (dash-dotted black lines). Results of the solution of the quantum master equation are shown for four different values of the quantum parameter $\zeta = 0.9\,,\ 1.1\,,\ 1.3\,,\ 1.6$. When compared to the classical curve the peaks appear gradually broadened, reduced in height, and shifted to lower detuning for increasing values of the quantum parameter ζ.

As expected, the discrepancy between the quantum mechanical and the classical result reduces with diminishing quantum parameter ζ. In this parameter regime, however, the full convergence towards the classical curve cannot be illustrated as the numerical costs become very large for small ζ, where the occupation numbers become large. The curves from the quantum master equation for large ζ seem to show features observed in the classical solution for a lower mechanical damping rate (or higher driving strength). The resonance at the second sideband emerges with increasing ζ and the gap between the first and the second sideband disappears (see also the blue and white contours in the attractor diagram).

2.5 Langevin Equations

We complement our analysis by comparing the results of the quantum master equation to numerical simulations of semiclassical Langevin equations that try to mimick the effects of quantum noise. To imitate both the zero-point fluctuations of the mechanical oscillator and the shot-noise inside the cavity, white noise terms, denoted by α_{in} and ξ, are added to the classical equations of motion:

$$\dot{\alpha} = [i(\Delta + g\frac{x}{x_{\mathrm{ZPF}}}) - \frac{\kappa}{2}]\,\alpha - i\alpha_L + \sqrt{\kappa/2}\,\alpha_{in} \tag{6}$$

$$\ddot{x} = -\omega_M^2 x + \frac{\hbar g}{m x_{\mathrm{ZPF}}}\,|\alpha|^2 - \Gamma_M\dot{x} + \sqrt{\hbar\omega_M\Gamma/m}\,\xi, \tag{7}$$

where $\langle\alpha_{in}\rangle = \langle\xi\rangle = 0$ and $\langle\alpha_{in}(t)\alpha_{in}^*(t')\rangle = \langle\xi(t)\xi(t')\rangle = \delta(t-t')$. The coefficients in front of the noise terms are chosen such that in the absence of optomechanical coupling we obtain the zero-point fluctuations, i.e. $\big\langle|\alpha|^2\big\rangle = 0.5$ away from optical resonance, and $\frac{m\omega_M^2}{2}\langle x^2\rangle = \frac{\hbar\omega_M}{4}$.

The results of a numerical simulation of the Langevin equations (6) and (7) are presented in figures 1(c) and (d) where again the oscillation energy (not including the mechanical zero-point energy) is plotted as a function of the detuning parameter. For negligible quantum fluctuations, i.e. for a small quantum parameter of $\zeta = 0.1$, the semiclassical curve recovers the classical solution of the attractor diagram as required for consistency. Increasing the quantum parameter allows to observe the complete transition into the quantum regime. The curves from the Langevin approach show the main features of the corresponding curves from the master equation approach (see figure 1(b)): The broadening of the peaks, the shift towards lower detunings and the emergence of the second sideband with increasing quantum parameter ζ.

Still, the Langevin approach can mimick the results from the master equation only partially. The approximation gets worse when dealing with low photon numbers and very large values of the quantum parameter ζ. In particular, the oscillation energy of the cantilever is overestimated by the semi-classical approach in the regions away from or in between the resonances. This is because the Langevin equation introduces artificial fluctuations of the radiation pressure force in the vacuum state. Indeed, $|\alpha|^2$ has a finite variance even in the ground state of the photon field, in contrast to $\hat{a}^\dagger \hat{a}$. To give a few numbers on the occupation numbers of the cavity for the parameters of figures 1(c) and (d) and $\zeta = 1.3$, we record that the photon number at $\Delta/\omega_M = -1$, $\Delta/\omega_M = 1.5$ and $\Delta/\omega_M = 2$ has dropped to values below 0.1 from a maximal value of 4.4 at the resonance. The semi-classical approach overestimates the quantum fluctuations, as becomes more and more apparent for large values of the quantum parameter. We observe that for $\zeta = 1.6$ the semi-classical curve of 1(c) deviates strongly from its fully quantum mechanical counterpart of figure 1(b) over the whole range of the detuning parameter.

Another inconsistency of the Langevin approach is the fact that the zero-point occupation of the cavity field does not lead to radiation pressure on the cantilever. To eliminate this effect, one might therefore try and replace the radiation pressure term of equation (7) by $\frac{\hbar g}{m x_{\mathrm{ZPF}}}(|\alpha|^2 - \frac{1}{2})$. The resulting curve in figure 1(d) is shifted towards higher detunings, but does not improve the comparison to the result from the quantum master equation. The manipulation of the radiation pressure term shows up in an easily visible artefact: the corresponding curve even shows an increase in the cantilever energy on the cooling side ($\Delta/\omega_M \lesssim -1$), where the actual cavity occupation should drop down to zero.

In summary, quantum fluctuations may significantly alter the features of self-induced oscillations in optomechanical systems. A semi-classical Langevin approach provides a useful tool to describe the quantum-classical crossover, complementing the master equation simulation of the full quantum dynamics.

3 Dynamical Interference in the "Photon Shuttle"

The standard approach to optomechanical systems is to record the transmission or reflection and thereby influence and detect the mechanical motion in steady

state. Going beyond this standard scheme, we want to ask what happens when the mechanical element is driven (periodically). It turns out that the most interesting features can be obtained when turning from the standard setup to a slightly different one, where a vibrating membrane is placed between two fixed end mirrors. The features reviewed in the following are discussed in more detail in a recent work of ours [10].

3.1 Model

We consider an optomechanical system with a membrane placed in the middle between two fixed mirrors, separating the cavity into two parts, Fig. 2a. This is different from the standard setup with a moveable end-mirror, but such a system was recently realized experimentally in [11]. The partially transparent membrane couples two modes a_L and a_R of the left and the right cavity half, respectively. The displacement $x(t)$ of the membrane changes the bare modes' frequency ω_0. Because of the coupling there is an avoided level crossing in the resonance frequency of the cavity, see Fig.2b. The system Hamiltonian reads

$$H_{sys} = \omega_0\hbar\left(1 - \frac{x(t)}{l}\right)a_L^\dagger a_L + \omega_0\hbar\left(1 + \frac{x(t)}{l}\right)a_R^\dagger a_R + g\hbar\left(a_L^\dagger a_R + a_R^\dagger a_L\right).$$

Here, $a_L^\dagger a_L$ and $a_R^\dagger a_R$ are the number operators for the left and right mode, respectively, l is the length of both cavity halves and g represents the optical coupling frequency. We assume that the membrane is driven with a mechanical frequency Ω and at an amplitude A around a mean position x_0, so the displacement reads:

$$x(t) = A\cos(\Omega t) + x_0.$$

Such a system may be termed a "photon shuttle": Photons will be transferred from the left half of the cavity to the right half by the mechanical driving. Here we will study in particular the regime where the timescale of photon exchange, governed by the optical coupling frequency g, becomes comparable to the timescale of the mechanical motion ($g \simeq \Omega$). In this case the system's dynamics can no longer be treated as quasi-static in terms of the hyperbola branches depicted in Fig. 2b (dotted). Instead, non-equilibrium photon dynamics driven by mechanical motion must be taken into account. We note that recently the optical coupling g has been significantly reduced [12] and is tunable down to 200 kHz at present. Thus, for typical mechanical drive in the range of 1 MHz, the regime $g \simeq \Omega$ is experimentally accessible.

To investigate the system, one may drive the left hand side of the cavity with a laser at frequency ω_L and examine the transmission $T(t)$ through the cavity at the right hand side. The coupling to external modes is treated in Markov approximation by a constant decay rate κ. Terms for dissipation and for the laser drive must be added to the system Hamiltonian. We consider the laser drive relative to the bare optical mode frequency ω_0 and define the detuning $\Delta_L = \omega_L - \omega_0$. To simplify the notation we express all length in terms of frequency: $\bar{A} = (\omega_0/l)A$, $\bar{x}_0 = (\omega_0/l)x_0$.

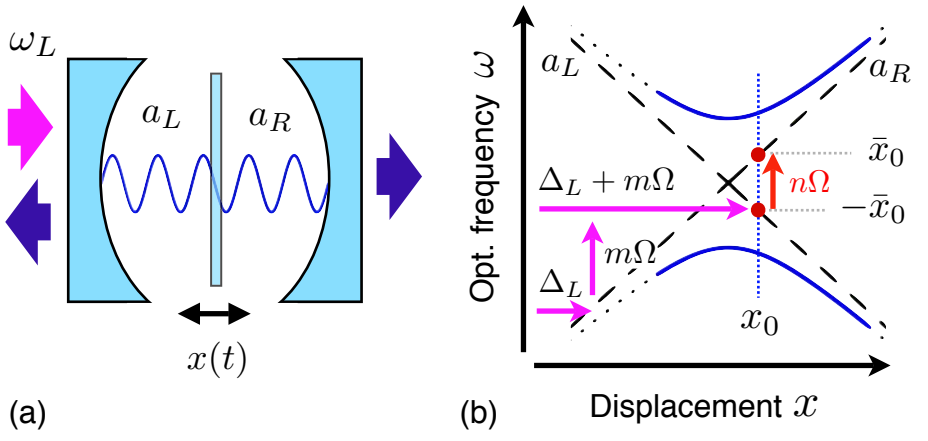

Fig. 2. The "photon shuttle". (a) Setup: a membrane placed inside a cavity couples two modes a_L, a_R. The left hand side is excited by a laser of frequency ω_L. The transmission to the right is recorded. (b) Resonance frequency as function of displacement. The membrane's motion linearly changes the bare mode frequencies (dashed). Due to the optical coupling (transmission through the membrane) there is an avoided crossing (dotted). The membrane is periodically driven around the mean position x_0. To see transmission, two multiphonon transitions are involved. First, excitation of the left cavity mode, Eq. (8). Second, transferring photons from the left to the right one, Eq. (9).

3.2 Physical Picture: Multiphonon Transitions

The observation of transmission through the cavity will be determined by two subsequent processes. First of all, the laser drive has to excite the cavity to insert photons into the left half. Secondly, the internal dynamics must be able to transfer these photons into the right mode such that transmission can be observed. In general, both processes are inelastic and therefore require energy to be transferred between the light field and the oscillating membrane. In the following, we restrict to the case of strong mechanical drive $\bar{A} \gg \Omega, g$ (see [10] for more details and other regimes).

Concerning the excitation process, the left mode is optically driven by the laser at frequency Δ_L. Due to the additional mechanical drive of the membrane, the left mode's frequency, $-\bar{x}(t) = -\bar{A}\cos(\Omega t) - \bar{x}_0$, is oscillating around its average value $-\bar{x}_0$. The resonance pattern of such a single periodically modulated optical mode, apart from the obvious resonance at $\Delta_L = -\bar{x}_0$, comprises mechanical sidebands due to multiphonon transitions. Thus, the condition to insert photons into the left mode of the cavity reads

$$\Delta_L + m\Omega = -\bar{x}_0, \tag{8}$$

see Fig. 2b. Here, $m\Omega$ is an adequate multiple of Ω. The width of the individual resonances is determined by the cavity decay rate κ. Note that due to the strong

drive the effective optical coupling between modes is very small and thus does not contribute.

The dynamics of the second process transferring photons from the left into the right mode turns out to be analogous to the one of a two state system, periodically driven through an avoided-crossing, where Landau-Zener (LZ) transitions [13,14] might occur. A LZ transition splits the photon state into a coherent superposition, the two amplitudes gather different phases and interfere the next time the system transverses the avoided crossing. For atomic systems such oscillations in the final state population, depending on the parameters of the drive, are known as Stueckelberg oscillations [15]. The same process might as well be depicted as a second multiphonon transition from the left mode with average frequency $-\bar{x}_0$ to the right one at $+\bar{x}_0$, see Fig. 2b. Thus, the second resonance condition becomes apparent, namely

$$n\Omega = 2\bar{x}_0. \tag{9}$$

3.3 Behaviour of the Optical Transmission in the Driven System

Rigorously, the transmission $T(t) = \kappa\langle a_R^\dagger(t)a_R(t)\rangle/(b^{in})^2$ is calculated using input-output theory, where b^{in} is the amplitude of the laser drive, and can be expressed as [10]

$$T(t) = \kappa^2 \left| \int_{-\infty}^{t} G(t,t')e^{-i\Delta_L t' - (\kappa/2)(t-t')}dt' \right|^2,$$

where the phase factor includes laser drive and cavity decay, while the Green's function $G(t,t')$ describes the amplitude for a photon to enter the cavity from the left at time t' and to be found in the right mode later at time t. The latter can be factorized $G(t,t') = \tilde{a}_R(t,t')e^{-i(\bar{A}/\Omega)\sin(\Omega t')}$, such that each factor describes one of the two processes discussed above. For the excitation, $e^{-i(\bar{A}/\Omega)\sin(\Omega t')} = \sum_m J_m(\bar{A}/\Omega)e^{-im\Omega t'}$ describes possible multiphonon transitions $m\Omega$, see (8), whose individual strength is determined by a Bessel function $J_m(\bar{A}/\Omega)$. Similarly, the strength of the second multiphonon transition $n\Omega$, originating from the internal dynamics described by $a_R(t,t')$, that is necessary to transfer photons from left to right, turns out to be determined by $J_n(2\bar{A}/\Omega)$. This second process and its dependence on $\bar{A}$ involves the physics of Stueckelberg oscillations as mentioned above.

In Fig. 3 we present numerical results for the time-averaged transmission ($\bar{A} \gg \Omega, g$) as a function of mean position x_0 and laser detuning Δ_L. This illustrates the two resonance conditions as well as the modulation by $\left|J_m(\bar{A}/\Omega)\right|$ and $\left|J_n(2\bar{A}/\Omega)\right|$. For $\Delta_L = 0$, the conditions (8) and (9) are met for $\bar{x}_0$ being a multiple of Ω. However, for the parameters used, $\left|J_{\pm1}(\bar{A}/\Omega)\right|$ is near a maximum while $\left|J_0(\bar{A}/\Omega)\right|$ is close to a minimum. Thus, the transmission for $\bar{x}_0 = 0$ is significantly smaller than for $\bar{x}_0 = \pm\Omega$. The periodicity of the Bessel function becomes clear from its asymptotic form for large arguments, $J_k(y) \simeq \sqrt{2/\pi y}\cos(y - k\pi/2 - \pi/4)$. For $m = -1$,

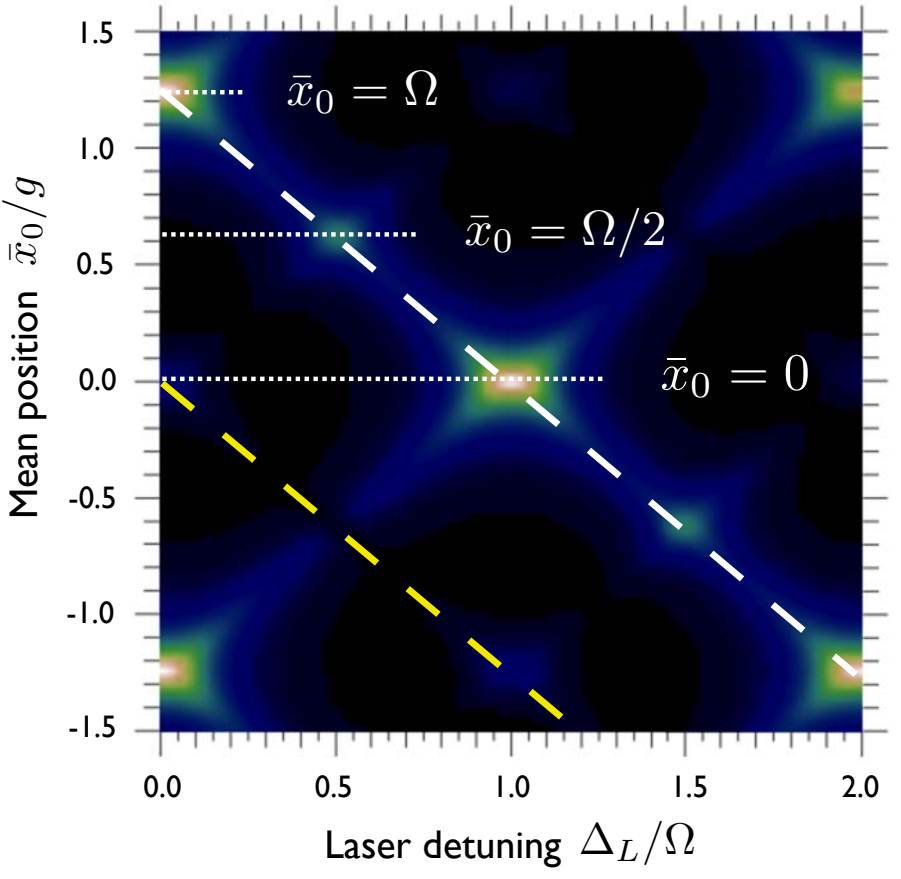

Fig. 3. Time-averaged transmission through an optical cavity with an oscillating partially transparent membrane in the middle. Transmission plotted as function of mean membrane position x_0 and laser detuning Δ_L. Further parameters are $\Omega/2\pi = 0.2g$, $\bar{A} = 54g$. Transmission can be observed if both resonance conditions (8) and (9) are met. Nevertheless, it is modulated by the product of two Bessel functions $\left|J_m(\bar{A}/\Omega)\right|$ and $\left|J_n(2\bar{A}/\Omega)\right|$ with appropriate indices according to (8) and (9). Dashed: $\bar{x}_0 = -\Delta_L - m\Omega$, see Eq. (8), with $m = -1$ (white) and $m = 0$ (yellow).

Eq. (8) is fulfilled along the white, dashed line. If we increase Δ_L we tune out of resonance and the transmission reduces. For $\Delta_L = \Omega/2$, (8) and (9) can be met for $\bar{x}_0$ being an *odd* multiple of $\Omega/2$, and so on. If we take into account the modulation by $\left|J_m(\bar{A}/\Omega)\right|$ and $\left|J_n(2\bar{A}/\Omega)\right|$ with the appropriate indices, we understand all the features of Fig. 3.

Even at low drive (small A), interesting features may be observed. In that regime, mechanically induced Rabi oscillations show up via an Autler-Townes splitting in the transmitted light. For more details, we refer the reader to [10].

Acknowledgments

We thank Björn Kubala and Jack Harris for collaborating on the quantum nonlinear dynamics and the photon shuttle, respectively. This work has been supported by the German Science Foundation (DFG) via NIM, SFB 631 and the Emmy-Noether program, as well as by the DIP and GIF programs.

References

1. Gröblacher, S., Hertzberg, J.B., Vanner, M.R., Cole, G.D., Gigan, S., Schwab, K.C., Aspelmeyer, M.: Demonstration of an ultracold micro-optomechanical oscillator in a cryogenic cavity. Nat. Phys. 5(7), 485–488 (2009)
2. Schliesser, A., Arcizet, O., Riviere, R., Anetsberger, G., Kippenberg, T.J.: Resolved-sideband cooling and position measurement of a micromechanical oscillator close to the Heisenberg uncertainty limit. Nat. Phys. 5(7), 509 (2009)
3. Marquardt, F., Girvin, S.M.: Optomechanics. Physics 2, 40 (2009)
4. Marquardt, F., Harris, J.G.E., Girvin, S.M.: Dynamical multistability induced by radiation pressure in high-finesse micromechanical optical cavities. Phys. Rev. Lett. 96, 103901 (2006)
5. Ludwig, M., Kubala, B., Marquardt, F.: The optomechanical instability in the quantum regime. New Journal of Physics 10, 095013 (2008)
6. Höhberger, C., Karrai, K.: Self-oscillation of micromechanical resonators. In: Nanotechnology 2004, Proceedings of the 4th IEEE conference on nanotechnology, p. 419 (2004)
7. Kippenberg, T.J., Rokhsari, H., Carmon, T., Scherer, A., Vahala, K.J.: Analysis of radiation-pressure induced mechanical oscillation of an optical microcavity. Phys. Rev. Lett. 95, 033901 (2005)
8. Metzger, C., Ludwig, M., Neuenhahn, C., Ortlieb, A., Favero, I., Karrai, K., Marquardt, F.: Self-induced oscillations in an optomechanical system driven by bolometric backaction. Phys. Rev. Lett. 101, 133903 (2008)
9. Murch, K.W., Moore, K.L., Gupta, S., Stamper-Kurn, D.M.: Observation of quantum-measurement backaction with an ultracold atomic gas. Nat. Phys. 4(7), 561–564 (2008)
10. Heinrich, G., Harris, J.G.E., Marquardt, F.: The photon shuttle: Landau-Zener-Stueckelberg dynamics in an optomechanical system (2009), arXiv:0909.2164
11. Thompson, J.D., Zwickl, B.M., Jayich, A.M., Marquardt, F., Girvin, S.M., Harris, J.G.E.: Strong dispersive coupling of a high-finesse cavity to a micromechanical membrane. Nature 452(7183), 72–75 (2008)
12. Sankey, J.C., Jayich, A.M., Zwickl, B.M., Yang, C., Harris, J.G.E.: Improved "position squared" readout using degenerate cavity modes. In: Cote, R., Gould, P.L., Rozman, M. (eds.) Proceedings of the XXI International Conference on Atomic Physics. World Scientific, Singapore (2008)
13. Zener, C.: Non-adiabatic crossing of energy levels. Proc. R. Soc. London A 137(Non-Adiabatic Crossing of Energy Levels), 696 (1932)
14. Landau, L.D.: On the theory of transfer of energy at collisions ii. Phys. Z. USSR 2, 46–51 (1932)
15. Stückelberg, E.C.G.: Theorie der unelastischen Stösse zwischen Atomen. Helv. Phys. Acta 5, 369–422 (1932)